Impact of centralized photovoltaic systems on utility power factor profile using the wavelet variability model

Michael Emmanuel, Student Member, IEEE, Ramesh Rayudu, Senior Member, IEEE, Ian Welch, Member, IEEE
School of Engineering & Computer Science
Victoria University of Wellington New Zealand
Email: {michael.emmanuel, ramesh.rayudu, ian.welch}@ecs.vuw.ac.nz

***Abstract*—This paper presents the impact of centralized photovoltaic (PV) systems with various power factor (PF) control schemes on the distribution feeder PF profile using the wavelet variability model (WVM). Centralized PV systems are large-scale plants ($>$ 1 MW), deployed at sites of prime solar resource availability and mostly at remote locations. The control strategies are fixed PF and PF schedule which adjusts the PF during day time. The WVM performs geographic smoothing of the irradiance data from a single point sensor across the entire PV plant in order to capture solar variability accurately and its associated interconnection effects on the grid. The IEEE-34 bus system with PV plants integrated close to feeder source, midpoint and end has been used as a case study. The test network contains bus coordinates used to map the feeder to the real world, and thus useful in capturing the locational value of PV systems.**

***Index Terms*—Geographical smoothing, photovoltaic system, power factor control, wavelet variability model.**

I. Introduction

Sustainable energy has become pivotal to underpin economic and social operations of every modern society. The need to operate a more reliable, secure and resilient electricity infrastructure currently drive the unprecedented evolution especially in the distribution and grid-edge domain of the electric power system (EPS) [1]–[3]. Other motivations include environmental concerns, increased customer participation in the electricity market and the critical need to comply with the demand for sustainable technologies uptake in the traditional EPS [1], [4].

Moreover, amongst the renewable distributed generation (DG) technologies, the solar photovoltaic system is now considered to be the most common DG integrated with the EPS [1], [5]. This can be attributed to various factors such as incentive programs, modularity, low maintenance and high power density per unit of weight [1]. However, the integration of PV-DG especially at high penetration can adversely impact the grid due to these five key characteristics of the solar resource. They include: low capacity factor, variability, uncertainty, location-peculiarity and non-synchronous generation [2]. Also, PV-DG integration could result in emergent behaviours such as increase in on-load tap changer operations, overvoltage, feeder power factor profile fluctuations and reverse power during low load conditions [2], [3].

978-1-5386-4950-3/17/$31.00 ©2017 IEEE

The PV-DG can be deployed as centralized or distributed (rooftop) systems with the EPS. However, in recent times due to favourable governmental decisions in providing cheap capital and competitive tenders ($<$ 50USD/MWh), centralized PV (i.e. utility-scale) plants have evolved at a more rapid rate than distributed PV units [6]. Therefore, the high penetration of utility-scale PV-DG in the grid requires an accurate modeling to capture its impacts, and thus provide distribution system planners and operator with the needed understanding in characterizing the grid operation.

The extant literature presents interconnection studies with average irradiance data to model PV-DG impacts on the grid as in [7]–[9]. A high frequency irradiance data and geographic smoothing over the entire PV plant footprint are pivotal to accurately characterize PV-DG impact on the grid.

This paper presents the locational value and impact of variability of centralized PV plants on the distribution feeder power factor (PF) profile using the wavelet variability model (WVM). Three deployment scenarios have been considered for the centralized plant, they are: single PV unit close to the feeder source, midpoint and end. Also, this paper presents the impact of these installations on the IEEE-34 bus feeder power factor profile which is needed for effective distribution planning and reliable operations.

II. Power factor control

Power factor (PF) is a key parameter in ensuring voltage stability in the distribution network. This is because at low PF below the utility minimum PF standards, there is a high tendency of voltage collapse occurrence [10]. For example, considering current flow in a three phase circuit given as:

$$I_{line} = \frac{P}{\sqrt{3}V_{line}Cos\theta} \tag{1}$$

$$I_{line} \propto \frac{1}{Cos\theta} \tag{2}$$

where I_{line} and V_{line} are line current and voltage. θ is the phase angle between the current and voltage, and $Cos\theta = PF$. From (2), at low PF the current increases, with adverse impact on the grid. The inefficiencies connected with low

PF operation include: high line losses, large voltage drops, big transmission lines, larger power plants, increased carbon footprint and penalty from authorities having jurisdiction over the grid (AHJ) [11].

Moreover, utilities do not only bill industrial and commercial customers for energy consumption and peak demand, but penalize them for low power factor operation [11], [12]. The AHJ provides tariffs or rules in order to govern the grid PF operating values within acceptable limits set by utilities (usually 0.85 - 1 leading/lagging) [13].

The feeder PF and load current at any particular point on the distribution grid are always changing due to the dynamic nature of most consumer loads [13]. Further, the voltage at any particular point away from the point of generation is prone to constant change due to voltage drops in impedances between the given point and generating source as depicted in Fig. 1. The required PF can be evaluated if the distribution system X/R ratio is given [13]. Feeders with a low X/R (small phase angle)

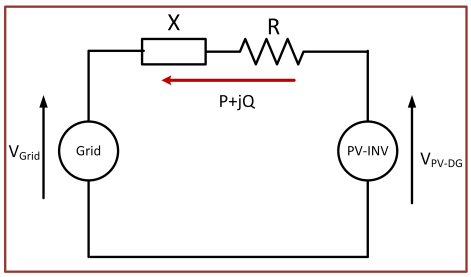

Fig. 1. PF control with feeder characteristics

ratio are prone to voltage rise while high X/R (high phase angle) ratio feeders experience less voltage rise . Generally, X/R ratio for distribution feeders ranges between 0.2 and 1.5. The PF can be calculated in terms of X/R ratio as follows [10], [14]:

$$Q = \left(\frac{1}{X/R}\right) * P \tag{3}$$

$$PF = cos\left[tan^{-}1\left(\frac{Q}{P}\right)\right] = cos\left(tan^{-}1\left(\frac{1}{X/R}\right)\right) \tag{4}$$

The presence of PV-DG can offset the load current and active power flowing in the grid, which invariably reduces the grid's PF. For instance, at unity PF with PV-DG the grid supplies less real power while the reactive power is kept constant. Also, at non-unity PF, the PV inverter has the capacity to supply both real (P(kW)) and reactive (Q(kVAr)) power (i.e. can behave as an inductor or a capacitor). The unused PV inverter capacity can be used to produce reactive power as shown in Fig. 2 [15], [16].

The amount of reactive power supply depends on the inverter rating (S(kVA)). In order to ensure an ample reactive power supply while maximizing the active power injection, the inverter is usually oversized by 10%, with $S = 1.1P_{PV-DG}$ [15], [17].

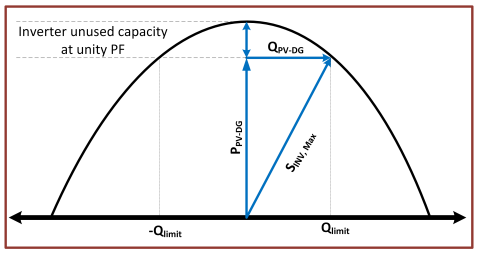

Fig. 2. PV inverter's quadrant operation

A. Power factor control methods

Two PF control strategies, fixed (unity) PF and PF schedule, have been considered in this paper. The PF schedule adjusts the PF during the day time as shown in Fig. 3. Distribution system planners and operators can use this schedule to control the inverter output to produce Vars for grid voltage support at certain periods during the day [18]–[20]. As shown in Fig.

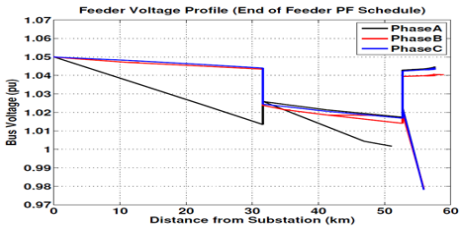

Fig. 3. A typical power factor schedule

3 the PF decreases during periods the peak sun hours which normally takes place in the middle of the day.

III. Load and Solar PV Modeling

A. Load modeling

Normalized annual commercial and residential load profiles (obtained from [5]) with a peak of 1 p.u. are incorporated into the test feeder as shown in Fig. 4. The annual load factor (LF) is given as [21]:

$$LF = \sum_{t=1}^{8760} \frac{p.u.\text{load demand (t)}}{8760} \tag{5}$$

The load factors are 0.7 and 0.4 for the commercial and residential profiles respectively.

B. Solar PV modeling

Accurate modelling of PV output variability is pivotal in order to capture and fully characterize its impact on the reliable operation of the grid. For this type of analysis, a high frequency solar irradiance data is required. However, variability of irradiance data from a single point sensor does not provide an accurate representation of solar variability across the entire PV plant [20].

To address this problem, this paper uses the WVM developed by Lave *et al*. [22], [23]. This model performs geographic

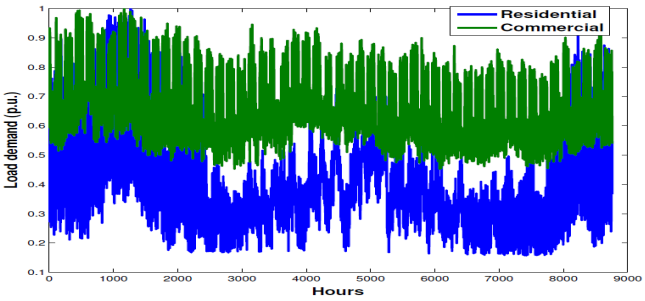

Fig. 4. Annual normalized commercial and residential profiles

smoothing of the irradiance data (obtained from [5]) with respect to the PV plant size and array dispersion. Other inputs to the WVM include the cloud speed scaling coefficient and plant density to produce the smoothed irradiance as shown in Fig. 5.

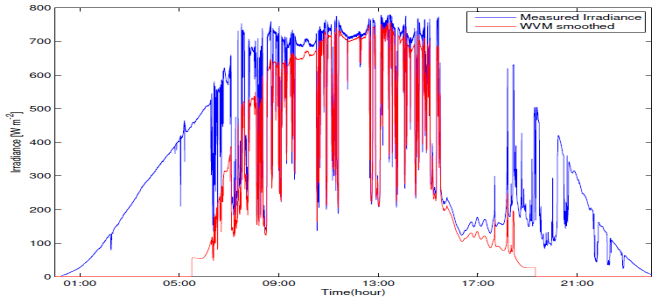

Fig. 5. WVM smoothed irradiance for the input irradiance and PV system

IV. Case Study

The modified IEEE-34 distribution feeder (Fig. 6) is used as a case study with an apparent load of 1769 kW and 1044 kVAr [24] and time-varying load profiles as shown in Fig. 4 are incorporated. The test system has two different operating voltages of 24.9 kV and 4.16 kV, load tap changer (LTC), voltage regulator (VREG), spot and distributed loads. Also, this is a long lightly loaded feeder located in Arizona, Phoenix [24]. The operating voltage constraint is from 0.95 to 1.05 p.u. Further, three different centralized PV scenarios are considered in this paper. They include: a single PV plant integrated close to the feeder source (812), midpoint (828) and end (836) as shown in Fig. 6. This diversity of PV deployment scenarios will enable distribution planners and operators to analyse the various impact and characterize grid operation.

A program written in Open-source distribution system simulator (OpenDSS) and MATLAB is used to obtain the optimal sizes (subject to voltage and loss contraints) at these locations. The optimal sizes are 1.45MW, 1.36MW and 1.27MW for buses 812, 828 and 836 respectively.

The OpenDSS has bus coordinates which is used to link each bus to its respective X and Y coordinates. The GridPV toolbox is then used to map the IEEE-34 bus on the Google

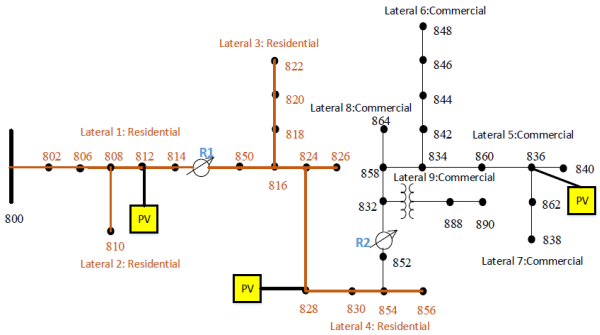

Fig. 6. Modified IEEE 34-bus test feeder. The modification refers to the presence of PV-DG

map (as shown in Fig. 7) through a function that converts circuit coordinates to GPS coordinates. With these coordinates, the geographic information system (GIS) is used to provide visualization of the circuit lines. The API for Google maps enables MATLAB to interact and download maps with data for a particular location and including elevation [20], [25].

Fig. 7 displays the IEEE-34 bus sited in Arizona as a typical example of GIS functionality. It shows the location of the substation, fixed capacitors, voltage regulators and phases.

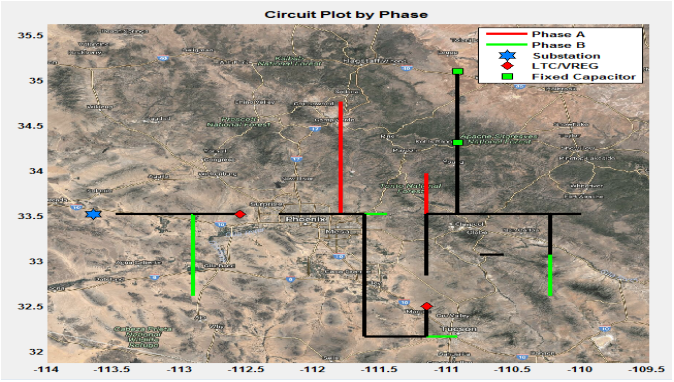

Fig. 7. IEEE-34 bus system in Arizona displayed on a Google Map (black line is for three phase lines used in connecting centralized PV systems)

V. Results and Discussion

The OpenDSS simulator coupled with MATLAB visual interface (through a COM interface) and GridPV toolbox are used to perform a high resolution time-series power flow analysis.

A. Basecase feeder PF profile during a typical week

As stated before, due to the dynamic nature of most loads, the feeder PF has a high tendency to always change at any given point on the grid. Figs. 8 and 9 show a typical basecase feeder PF profile and contour during the sample week. The PF color contour aids visualization of PF values at different circuit sections, which can be very useful at utility control centres to detect possible violations.

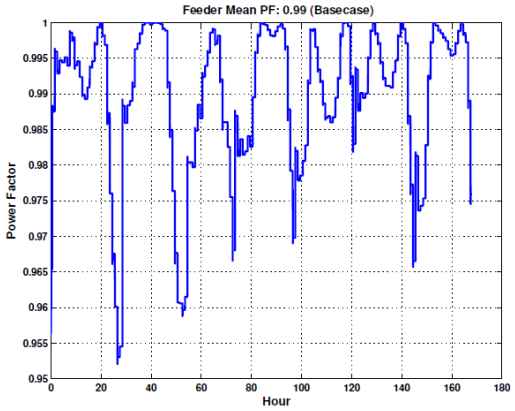

Fig. 8. Basecase feeder PF profile in the sample week

In Fig. 8, the PF varies from 0.952 to 1 with the feeder mean PF of 0.9 for a typical sample week. In Fig. 9, the PF ranges

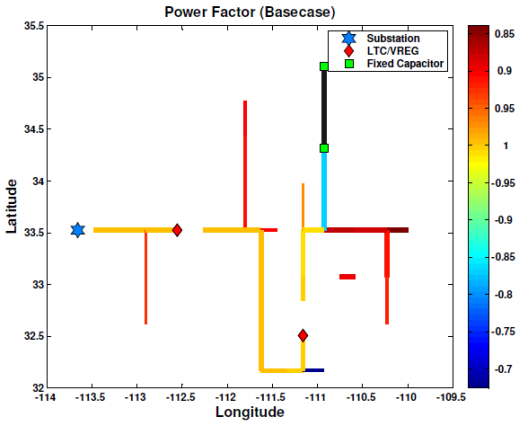

Fig. 9. Basecase feeder PF contour plot

from lagging values of 0.7 to 0.95 and leading values of 0.85 to unity. Branches close to the substation and feeder midpoint operate at high leading PF values with mostly residential loads. Branches towards the end of feeder operate between leading and lagging PF.

B. Optimal size centralized PV integrated close to the start of feeder (SOF)

Figs. 10 and 11 respectively show the impact of PV plant operating with PF schedule and unity PF placed at bus 812 on the feeder PF profile. Apart from the effect of the inherent variability of loads on the PF profile, PV system integration increases its variation during the sample week. This occurs mostly during the peak sun hour around mid-day when the PV unit injects the highest amount of power into the grid.

In Fig. 10, the PF profile reduces from a minimum basecase value of about 0.952 to 0.72 after PV integration operating with a PF schedule. At unity PF (Fig. 11), the net feeder PF dropped to 0.4 at hour 60 on the simulation hour. More so, for both control schemes the feeder mean PF reduced from a

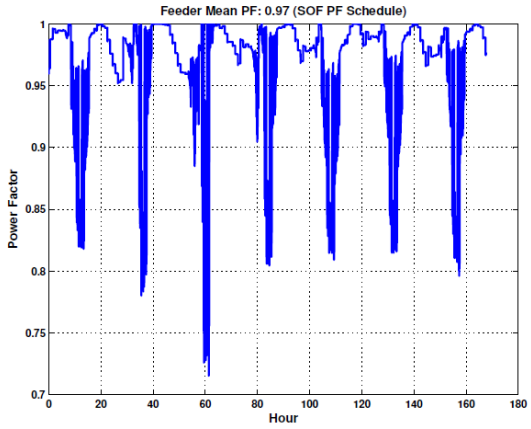

Fig. 10. PV plant operating with PF schedule close to the SOF

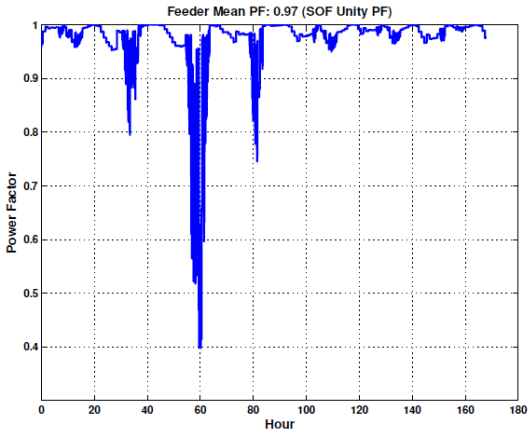

Fig. 11. PV plant operating at unity PF close to the SOF

basecase value of 0.99 to 0.97. Further, as shown in contour plot (Fig. 12), the PF decreases around the PV location and along the feeder branches.

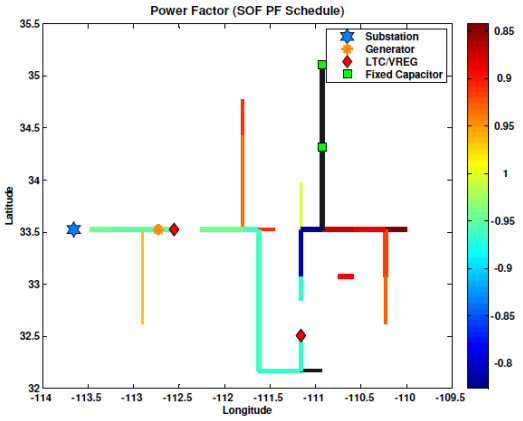

Fig. 12. feeder PF contour plot for PV close to the SOF

C. Optimal size centralized PV integrated close to the mid-point of feeder (MOF)

The PV plant deployed close to the midpoint shows an improvement over the plant close to the start of feeder as depicted in Figs. 13 and 14. For the PF schedule control

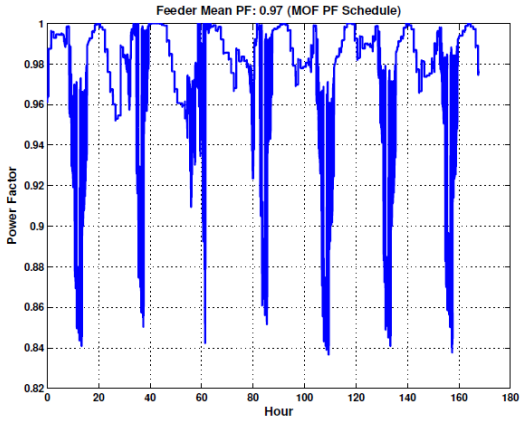

Fig. 13. PV plant operating with PF schedule close to the MOF

method, the minimum PF value during the sample week was around 0.84 with a mean of 0.97 while at unity PF the value dropped to 0.55 with a mean of 0.98.

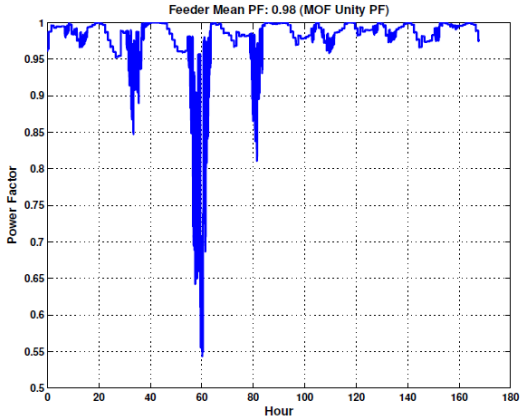

Fig. 14. PV plant operating at unity PF close to the MOF

D. Optimal size centralized PV integrated close to the end of feeder (EOF)

The centralized PV plant integrated close to the EOF outperformed the previous PV scenarios. For PF schedule control, the minimum PF value during the sample week was above 0.86 with a mean of 0.98 while at unity PF the minimum value dropped to 0.6 with a mean of 0.98.

VI. Conclusion

Power factor remains a critical parameter in maintaining voltage stability in the electricity grid. Apart from the effect of customer load on PF variation, the integration of variable centralized PV plants further increases the PF variability which

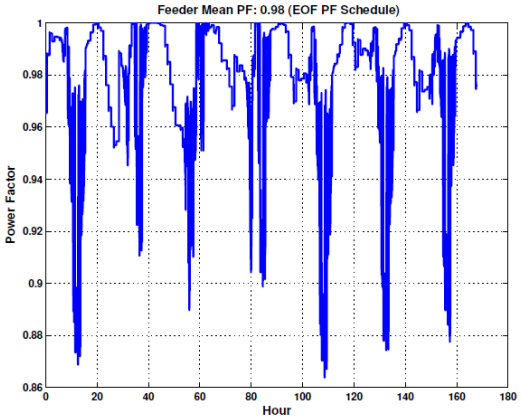

Fig. 15. PV plant operating with PF schedule close to the EOF

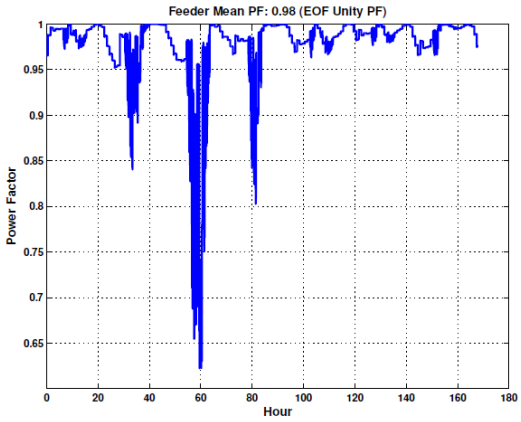

Fig. 16. PV plant operating at unity PF close to the EOF

must be managed by the utility. Moreover, due to inefficiencies associated with low PF operation, utilities penalizes customers for power consumption at low PF by proving tariffs. In addition, the centralized PV integrated close to the EOF resulted in the least amount of PF reduction in comparison with other deployment scenarios. Also, the PF schedule control scheme led to less reduction in PF variation than the unity PF scheme. The PF schedule method has the benefit of operating at PF close to unity in the mornings and evenings when PV generation is low in order to provide voltage support.

Acknowledgment The authors gratefully acknowledge the support of Victoria University for this work through the VUW Research Trust.

References

[1] M. Emmanuel and R. Rayudu, "The impact of single-phase grid-connected distributed photovoltaic systems on the distribution network using P-Q and P-V models," *International Journal of Electrical Power & Energy Systems*, vol. 91, pp. 20–33, 2017.

[2] J. Cochran, D. Paul, B. Speer, and M. Miller, "Grid integration and the carrying capacity of the U.S. grid to incorporate varaiable renewable energy," Tech. Rep., 2015.

[3] M. Begovic, I. Kim, D. Novosel, J. R. Aguero, and A. Rohatgi, "Integration of Photovoltaic Distributed Generation in the Power Distribution Grid." IEEE Computer Society, 2012, pp. 1977–1986.
[4] M. Emmanuel, D. Akinyele, and R. Rayudu, "Techno-economic analysis of a 10 kWp utility interactive photovoltaic system at Maungaraki school, Wellington, New Zealand," *Energy*, vol. 120, no. Supplement C, pp. 573–583, 2017.
[5] "Electric Power Research Institute (EPRI), OpenDSSWiki." [Online]. Available: https://sourceforge.net/p/electricdss/
[6] "Trends 2016 in Photovoltaic Applications, Survey Report of Selected IEA Countries between 1992 and 2015," International Energy Agency, Tech. Rep.
[7] C. Paravalos, E. Koutroulis, V. Samoladas, T. Kerekes, D. Sera, and R. Teodorescu, "Optimal Design of Photovoltaic Systems Using High Time-Resolution Meteorological Data," *IEEE Transactions on Industrial Informatics*, vol. 10, no. 4, pp. 2270–2279, 2014.
[8] G. Mokryani, A. Majumdar, and B. C. Pal, "Probabilistic method for the operation of three-phase unbalanced active distribution networks," *IET Renewable Power Generation*, vol. 10, no. 7, pp. 944–954, 2016.
[9] D. Q. Hung, N. Mithulananthan, and K. Y. Lee, "Determining PV Penetration for Distribution Systems With Time-Varying Load Models," *IEEE Transactions on Power Systems*, vol. 29, no. 6, pp. 3048–3057, 2014.
[10] M. H. Bollen and F. Hassan, *Integration of distributed generation in the power system*. John wiley & sons, 2011, vol. 80.
[11] "G. lee, "How PV Grid-Tie Inverters Can Zap Utility Power Factor," Renewable Energy World, Oct. 15, 2009."
[12] "Power Factor and Grid-Connected Photovoltaics," Tech. Rep., 2015.
[13] "IEEE Application Guide for IEEE Std 1547TM, IEEE Standard for Interconnecting Distributed Resources with Electric Power Systems ," 2008.
[14] S. Hong, "A Mitigation Strategy to Address Voltage Flicker due to the Cloud Cover Effect." IEEE Power and Energy Society General Meeting, 2014.
[15] Y. Liu, J. Bebic, B. Kroposki, J. De Bedout, and W. Ren, "Distribution system voltage performance analysis for high-penetration PV," in *Energy 2030 Conference, 2008. ENERGY 2008. IEEE*. IEEE, 2008, pp. 1–8.
[16] M. Zuercher-Martinson, "Smart PV inverter benefits for utilities," Tech. Rep., 2011.
[17] M. Emmanuel and R. Rayudu, "Equipment loading and voltage unbalance in the distribution network with distributed PVs," in *2016 IEEE Innovative Smart Grid Technologies - Asia (ISGT-Asia)*, Nov 2016, pp. 9–14.
[18] M. J. Reno and K. Coogan, ""Grid Integrated Distributed PV (GridPV)," Sandia National Laboratories SAND2013-6733, 2013." Tech. Rep.
[19] R. J. Broderick, J. E. Quiroz, M. J. Reno, A. Ellis, J. Smith, and R. Dugan, "Time Series Power Flow Analysis for Distribution Connected PV Generation, Sandia National Laboratories SAND2013-0537, 2013." Tech. Rep.
[20] M. Emmanuel, R. Rayudu, and I. Welch, "Impacts of power factor control schemes in time series power flow analysis for centralized PV plant using wavelet variability model," vol. PP, no. 99, pp. 1–1, 2017.
[21] M. Emmanuel, R. K. Rayudu, and I. Welch, "Grid capacity released analysis and incremental addition computation for distribution system planning," *Electric Power Systems Research*, vol. 152, pp. 105–121, 2017.
[22] M. Lave, M. J. Reno, and R. J. Broderick, "Characterizing local high-frequency solar variability and its impact to distribution studies," *Solar Energy*, vol. 118, pp. 327–337, 2015.
[23] M. Lave, J. Kleissl, and J. S. Stein, "A Wavelet-Based Variability Model (WVM) for Solar PV Power Plants," *IEEE Transactions on Sustainable Energy*, vol. 4, no. 2, pp. 501–509, April 2013.
[24] "Distribution System Analysis Subcommittee, IEEE 34 node test feeder," Tech. Rep. [Online]. Available: https://ewh.ieee.org/soc/pes/dsacom/testfeeders/
[25] "Google. Google Maps API Family." [Online]. Available: https://code.google.com/apis/maps/index.html